

Interlaminar Fracture Toughness Estimation of Aerospace Composites by Weighted Residual Approach

V. Alfred Franklin^{a,1} and T. Christopher^b

^a Faculty of Mechanical Engineering, Sardar Raja College of Engineering, Alangulam, Tirunelveli, India

^b Faculty of Mechanical Engineering, Government College of Engineering, Tirunelveli, India

¹ frank_vin@ yahoo.com

УДК 539.4

Оценка межслойной вязкости разрушения аэрокосмических композитных материалов методом взвешенных невязок

В. Альфред Франклин^а, Т. Кристофер^б

^а Технический колледж им. Сардара Раджи, Ангулам, Тирунвелли, Индия

^б Государственный технический колледж, Тирунвелли, Индия

Исследована межслойная вязкость разрушения образцов, представляющих собой двухконсольную балку, из упрочненных волокнами углепластиковых композитов с учетом поворота вершины трещины. При измерении нагрузок, перемещений и длины трещин могут иметь место значительные погрешности. Для уменьшения разброса данных предлагается использовать метод взвешенных невязок, позволяющий минимизировать влияние погрешностей измерения на оценку критической энергии разрушения и получить для каждого образца свое значение.

Ключевые слова: конструкция самолета, образец в виде двухконсольной балки, расслоение, углепластик с эпоксидной смолой, углепластики типа РЕЕК, PES и РЕК-С.

Notation

- a – crack length
- B – width of the DCB specimen
- C – compliance of the specimen
- E – longitudinal tensile modulus (the Young modulus)
- G – strain energy release rate (SERR)
- G_{Ic} – fracture toughness or critical strain energy release rate
- $2h$ – specimen thickness
- I – moment of inertia
- K – rotational spring stiffness
- n – number of fracture data
- P – applied load on both sides of the specimen
- δ – crack mouth opening displacement
- Π – potential energy

Introduction. Preventing failure of composite material systems has been an important issue in engineering design. There are two types of physical failures that occur in laminated composite structures and interact in complex manner are intralaminar and interlaminar failures. Intralaminar failure is manifest in micromechanical components of the lamina such as fiber breakage, matrix cracking, and debonding of the fiber–matrix interface. Generally, aircraft structures made of fiber reinforced composite materials are designed such that the fibers carry the bulk of the applied load. Interlaminar failure such as delamination refers to debonding of adjacent lamina. The possibility that intralaminar and interlaminar failure occur in structural components is considered a design limit, and establishes restrictions on the usage of full potential of composites. Due to the lack of through-the-thickness reinforcement, structures made from laminated composite materials and adhesively bonded joints are highly susceptible to failure caused by interfacial crack initiation and growth. The delamination phenomenon in a laminated composite structure may reduce the structural stiffness and strength, redistribute the load in a way that the structural failure is delayed, or may lead to structural collapse. Therefore, delamination is not necessarily the ultimate structural failure, but rather it is the part of the failure process which may ultimately lead to loss of structural integrity.

Most of the components on the aircraft are increasingly being replaced with composite materials. The main attraction is the effective reduction in mass with a comparative increase in stiffness, strength, fatigue and impact resistance, thermal conductivity and corrosion resistance. Through these replacements, the structural weight can be reduced, which will in turn lead to a more economical commercial aircraft [1]. The major structural applications for fiber-reinforced composites are in the field of military and commercial aircrafts, for which weight reduction is critical for higher speeds and increased payloads. Ever since the production application of boron fiber-reinforced epoxy skins for F-14 horizontal stabilizers, the use of fiber-reinforced polymers has experienced a steady growth in the aircraft industry. Carbon fiber-reinforced epoxy has become the primary material in many wings, fuselage, and empennage components. The structural integrity and durability of these early components have built up confidence in their performance and prompted developments of other structural aircraft components, resulting in an increasing amount of composites being used in military aircrafts. The F-22 fighter aircraft also contains nearly 25% by weight of carbon fiber-reinforced polymers. The outer skin of B-2 and other stealth aircrafts is almost all made of carbon fiber-reinforced polymers. The stealth characteristics of these aircrafts are due to the use of carbon fibers, special coatings, and other design features that reduce radar reflection and heat radiation [2].

Airbus was the first commercial aircraft manufacturer to make extensive use of composites in their A310 aircraft. The composite components weighed about 10% of the aircrafts weight and included such components as the lower access panels and top panels of the wing leading edge, outer deflector doors, nose wheel doors, main wheel leg fairing doors, engine cowling panels, elevators and fin box, leading and trailing edges of fins, flap access doors, flap track fairings, rear and forward wingbody fairings, nose radome, pylon fairings, cooling air inlet fairings, tail leading edges, upper surface skin panels above the main wheel bay, glide slope antenna cover, and rudder. The composite vertical stabilizer, which is 7.8 m wide by 8.3 m high at the base, is about 400 kg lighter than the aluminium vertical stabilizer previously used [3]. The Airbus A320 was the first commercial aircraft to use an all-composite tail, which includes the tail cone, vertical stabilizer, and horizontal stabilizer. The composite usage in Airbus A380 during last decade was about 25% of its weight. Among the major composite components in A380 are the rear-pressure bulkhead (a dome-shaped partition that separates the passenger cabin from the rear part of the plane that is not pressurized), the central torsion box (which links the left and right wings under the fuselage), the tail, and the flight control surfaces, such as the spoilers, flaps, and ailerons.

Starting with Boeing 777, Boeing has started making use of composites in the empennage (which include vertical stabilizer, horizontal stabilizer, elevator, and rudder), most of the control surfaces, engine cowlings, and fuselage floor beams (see Fig. 1). About 10% of Boeing 777's structural weight is made of carbon fiber-reinforced epoxy. About 50% of the structural weight of Boeings next line of airplanes, called the Boeing 787 Dreamliner, will be made of carbon fiber-reinforced composites. Two of the major composite components in 787 will be the fuselage and the forward section, both of which will use carbon fiber-reinforced epoxy as the major material of construction. Publications by Boeing [4, 5] and NASA [6] reveal that the residual strength prediction of composite structures with discrete source damage is an area in which more research is needed.

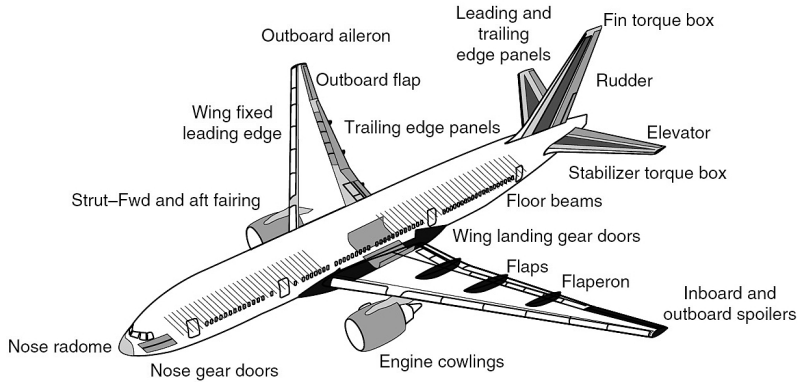


Fig. 1. Use of laminated composites in Boeing 777 [2].

The present study aims to derive a simple expression for critical fracture energy based on weighted residual approach, considering non-zero slope at the crack tip of the DCB specimen and to demonstrate its potentiality by comparing the calculated critical load, P_{cr} , and the corresponding displacement, δ_{cr} , for the measured crack length.

1. Data Reduction for Critical Fracture Energy. Tamuzs et al. [7] investigated the dependence of crack growth resistance curves on the geometry of DCB specimens was by for unidirectional carbon/epoxy composite laminates and they modified the beam theory to calculate the energy release rate in terms of $P-\delta$ record. Usually the energy release rate in a DCB specimen is defined as

$$G = -\frac{\partial \Pi}{B \partial a}. \quad (1)$$

The potential energy of a linearly elastic system is equal to

$$\Pi = \frac{1}{2} \int_v \sigma_{ij} \varepsilon_{ij} dv - \int_0^u P(u) du, \quad (2)$$

where σ_{ij} and ε_{ij} are the stress and strain, v is the volume, and $P(u)$ is the force applied, which is a function of displacement. The first term is an energy stored in the linearly elastic body and the second one is the work produced by the applied external force. The displacement u is a full opening of the DCB specimen at the point, where P is applied. The first term is also expressed through the force acting on the system

$$\Pi = \frac{1}{2} Pu - \int_0^u P(u) du. \quad (3)$$

From Eqs. (1) and (3), the SERR can be written by

$$G = \frac{P^2}{2B} \frac{\partial C}{\partial a}. \quad (4)$$

Considering root rotation at crack tip, the compliance C is given by

$$C = \frac{\delta}{P} = \frac{2}{3} \frac{a^3}{EI} + \frac{2}{K} a^2. \quad (5)$$

Using Eq. (4) and eliminating K in Eq. (5), one gets [8, 9]

$$G_{1c} = \frac{P^2 a^2}{3BEI} + \frac{P\delta}{Ba}. \quad (6)$$

The critical load P_{cr} at the initiation of the delamination growth in DCB specimen can be determined as

$$P_{cr} = \left(G_{1c} \left\{ \frac{a^2}{BEI} + \frac{2}{K} \frac{a}{B} \right\}^{-1} \right)^{1/2}. \quad (7)$$

1.1. **Weighted Residual Approach to Evaluate G_{1c} .** There may be chances to prone errors in the parameters viz., load P , displacement δ , and crack length a as they are measured quantities. To minimize the scatter in measurements, the weighted residual approach is used to derive the fracture energy. From Eq. (6), one can write the error E_{rr} as

$$E_{rr} = \sum_{i=1}^n \left(\frac{P_i^2 a_i^3}{3BEI} + \frac{P_i \delta_i}{B} - G_{1c} a_i \right)^2. \quad (8)$$

The energy release rate can be maxima when

$$\frac{\partial E_{rr}}{\partial G_{1c}} = 0. \quad (9)$$

From Eqs. (8) and (9), one gets the critical energy release rate as

$$G_{1c} = \sum_{i=1}^n \left(\frac{P_i^2 a_i^4}{3BEI} + \frac{P_i \delta_i a_i}{B} \right) \bigg/ \sum_{i=1}^n a_i^2. \quad (10)$$

Similarly the rotational spring constant K can be obtained from

$$\frac{1}{K} = \sum_{i=1}^n \left(\frac{\delta_i}{P_i} - \frac{2}{3} \frac{a_i^3}{EI} \right) a_i^2 \bigg/ \sum_{i=1}^n 2a_i^4. \quad (11)$$

Using Eq. (11) in Eq. (7), the critical load P_{cr} at the initiation of the delamination growth in DCB specimen can be obtained. The displacement δ_{cr} corresponding to the load P_{cr} can be obtained from Eq. (5).

2. Results and Discussions. Fracture analysis has been carried out on the double cantilever beam specimens made of carbon-fibre/PEEK, carbon/polyether sulphone, carbon/epoxy, and carbon/PEK-C composites and compared with the published results. The tensile opening (mode I) fracture energy G_{Ic} is evaluated from the load–displacement data for DCB specimens with cracks, using weighted residual approach derived from displacement method. The results (Figs. 2–9) obtained by this approach is in good agreement with published test results.

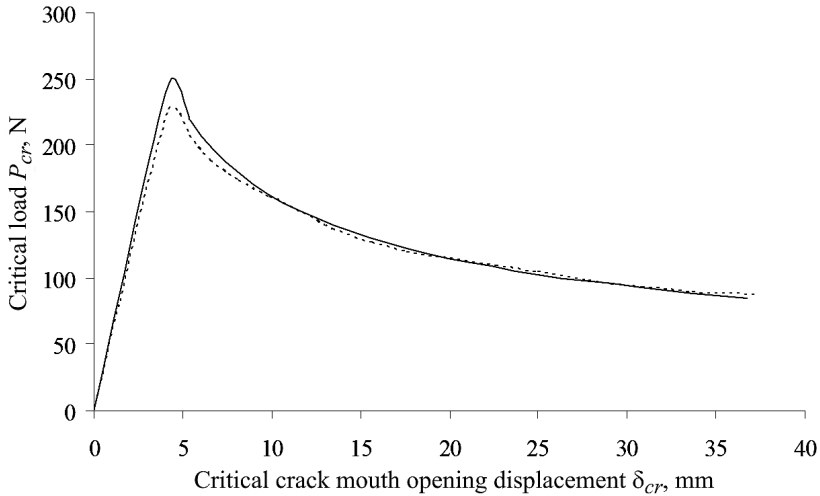


Fig. 2. Comparison of load–displacement curves of DCB specimens made of carbon/PEEK [10]. (Here and in Figs. 3–9: dash line corresponds to test results and solid line – present analysis.)

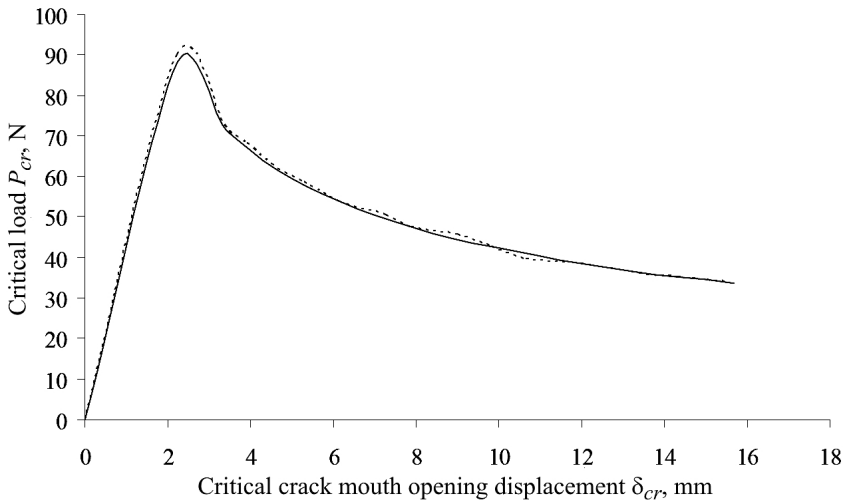


Fig. 3. Comparison of load–displacement curves of DCB specimens made of carbon/epoxy [10].

The rotational stiffness of the support at the crack tip of the DCB specimen, K , is determined by substituting the initially recorded fracture data (viz. load P , displacement δ , and crack size a) from the loading/unloading curves, and the Young modulus E of the material in Eq. (11). Using the fracture data of the DCB specimen, the value of G_{Ic} was calculated using Eq. (10). This modified weighted residual method gives a unique value of G_{Ic} and is found to be in good agreement with published results (see Table 1). If the stiffness of is too large, the effect of K on G_{Ic} may not significant in that particular case.

Table 1

Comparison of Fracture Energy of Carbon Fiber-Reinforced Composites

Material	Critical energy release rate G_{Ic} , J/m ²			
	Eq. (6)	Cubic law [8]	Power law [8]	Present analysis Eq. (10)
Carbon/PEEK [10]	2006.37	2051.68	2149.03	2045.48
Carbon/epoxy [10]	262.73	261.60	287.90	261.56
Carbon/PES [11]	2150.64	2121.76	2230.22	2298.68
T300-634 DDS [12]	642.13	641.01	641.80	597.26
Carbon/epoxy [13]	364.07	361.60	428.94	355.36
CYCOM-982 [14]	262.33	264.10	271.79	261.47
APC-2 [14]	1563.81	1582.46	1655.85	1578.25
Carbon/PEK-C [15]	877.33	873.70	875.12	899.09

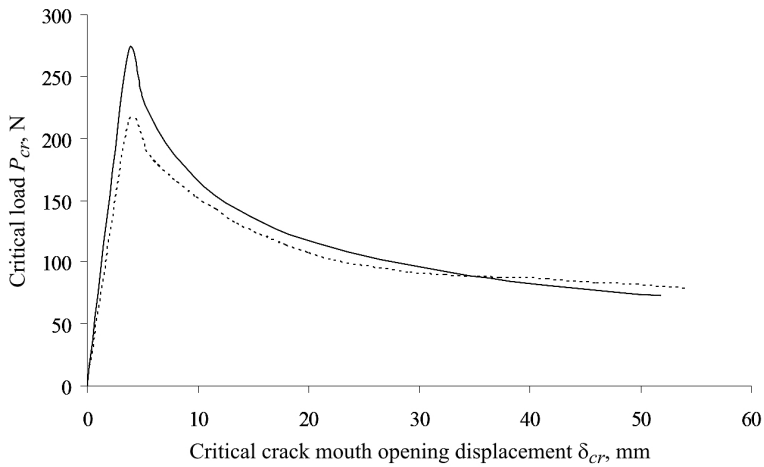


Fig. 4. Comparison of load–displacement curves of DCB specimens made of carbon/PES [11].

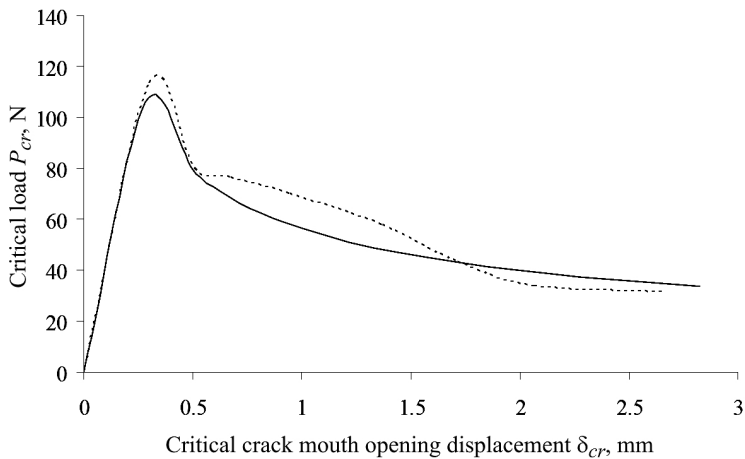


Fig. 5. Comparison of load–displacement curves of DCB specimens made of T300-634 DDS [12].

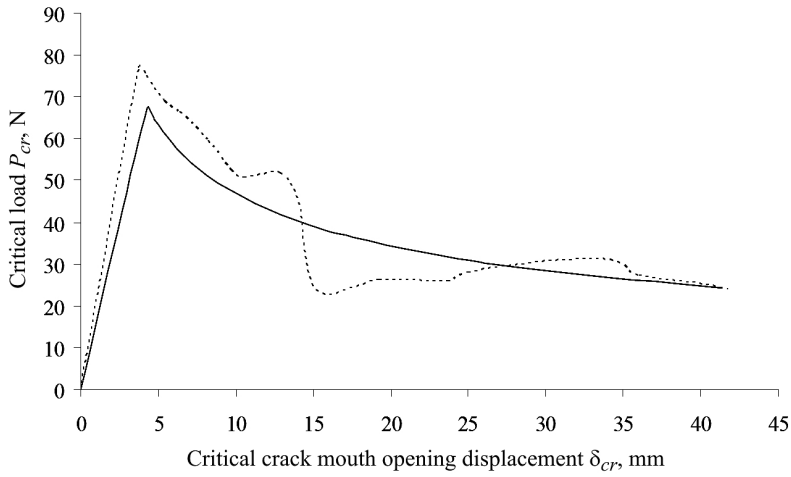


Fig. 6. Comparison of load–displacement curves of DCB specimens made of carbon/epoxy [13].

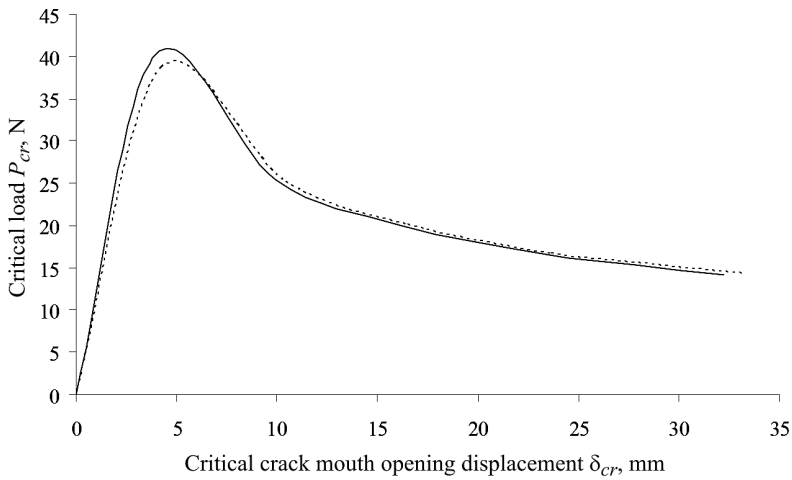


Fig. 7. Comparison of load–displacement curves of DCB specimens made of CYCOM-982 [14].

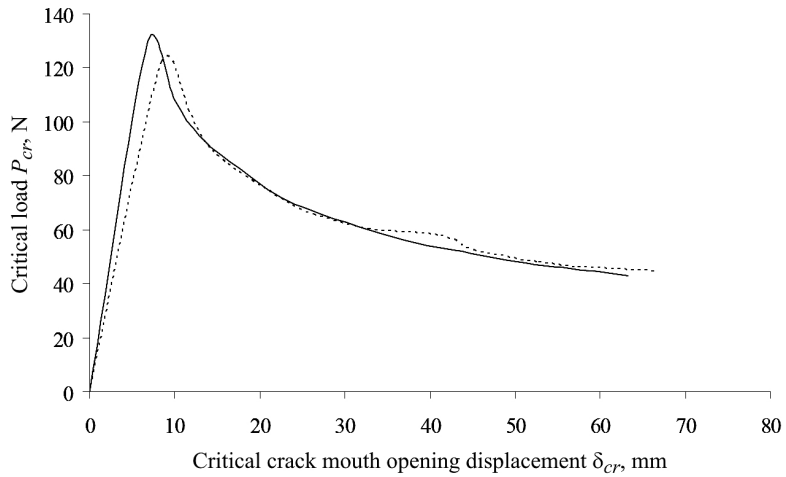


Fig. 8. Comparison of load–displacement curves of DCB specimens made of APC-2 [14].

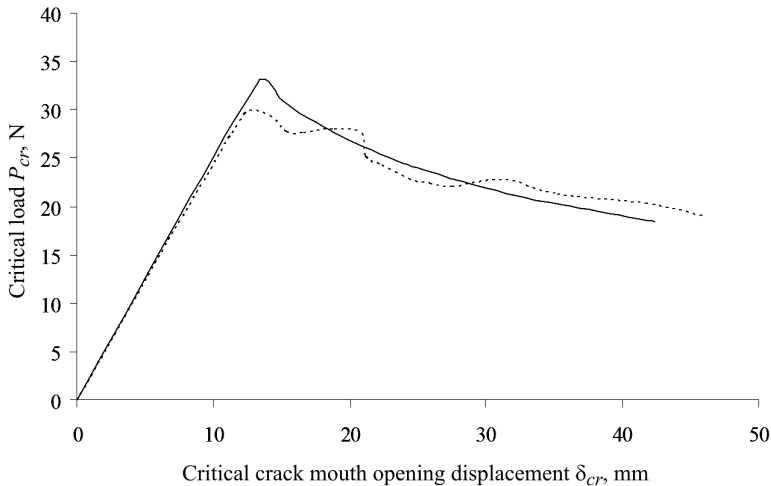


Fig. 9. Comparison of load–displacement curves of DCB specimens made of carbon/PEK-C [15].

3. Concluding Remarks. To minimize the error in measurements of load, displacement and crack length, weighted residual equation for determination of energy release rate was derived in the present study. The critical fracture energy G_{Ic} was evaluated based on the proposed approach gives a unique value of G_{Ic} for the particular specimen which is in good agreement with the published test results. From the Figs. 2–9, it is observed that of $P-\delta$ curve by the present approach is almost in line with the experimental results.

Резюме

Досліджено міжшарову в'язкість руйнування зразків, що являють собою двоконсольну балку, зі зміцнених волокнами вуглепластикових композитів з урахуванням повороту вершини тріщини. При вимірюванні навантажень, переміщень та довжини тріщин можуть мати місце значні похибки. Для зменшення розкиду даних пропонується використовувати метод зважених нев'язок, що дозволяє мінімізувати вплив похибок при вимірюванні на оцінку критичної енергії руйнування і отримати для кожного зразка своє значення.

1. I. E. A. Aghachi and E. R. Sadiku, “Integrity of glass/epoxy aircraft composite part repaired using five different methods,” *Int. J. Eng. Sci. Technol.*, **5**, No. 1, 178–183 (2013).
2. P. K. Mallick, *Fiber-Reinforced Composites: Materials, Manufacturing, and Design*, CRC Press, New York (2007).
3. C. Soutis, “Carbon fiber reinforced plastics in aircraft applications,” *Mater. Sci. Eng. Part A*, **412**, 171–176 (2005).
4. T. H. Walker, L. B. Ilcewicz, D. R. Polland, and C. C. Poe, Jr., “Tension fracture of laminates for transport fuselage. Part II: Large notches,” in: Proc. of the Third NASA/DoD ACT Conf., NASA CP-3178, Part 2 (1992), pp. 727–758.
5. T. H. Walker, L. B. Ilcewicz, D. R. Polland, et al., “Tension fracture of laminates for transport fuselage. Part III: Structural configurations,” in: Proc. of the Fourth NASA/DoD ACT Conf., NASA CP-3229, Part 1 (1993), pp. 863–880.

6. J. T. Wang, C. C. Poe, Jr., D. R. Ambur, and D. W. Sleight, "Residual strength prediction of damaged composite fuselage panel with *R*-curve method," *Compos. Sci. Technol.*, **66**, 2557–2565 (2006).
7. V. Tamuzs, S. Tarasovs, and U. Vilks, "Progressive delamination and fiber bridging modelling in double cantilever beam composite specimens," *Eng. Fract. Mech.*, **68**, 513–525 (2001).
8. V. Alfred Franklin and T. Christopher, "Fracture energy estimation of DCB specimens made of glass/epoxy: an experimental study," *Adv. Mater. Sci. Eng.*, **2013**, Article ID 412601 (2013).
9. V. Alfred Franklin and T. Christopher, "Generation and validation of crack growth resistance curve from DCB specimens: an experimental study," *Strength Mater.*, **45**, No. 6, 674–683 (2013).
10. B. N. Rao, and A. R. Acharya, "Evaluation of fracture energy, using a double cantilever beam fibre composite specimen," *Eng. Fract. Mech.*, **51**, 317–322 (1995).
11. S. Hashemi, A. J. Kinloch, and J. G. Williams, "Mechanics and mechanism of delamination in poly(ether sulphone)-fiber composite," *Compos. Sci. Technol.*, **37**, 429–462 (1990).
12. L. Ye, "Evaluation of mode-I interlaminar fracture toughness for fiber-reinforced composite materials," *Compos. Sci. Technol.*, **43**, 49–54 (1992).
13. V. Q. Bui, E. Marechal, and H. Nguyen-Dang, "Imperfect interlaminar interfaces in laminated composites: delamination with the *R*-curve effect," *Compos. Sci. Technol.*, **60**, 2619–2630 (2000).
14. J. W. Gillespie, Jr., L. A. Carlsson, R. B. Pipes, et al., *Delamination Growth in Composite Materials*, NASA-CR 178066 (1986), pp. 1–208.
15. J. Zhou, T. He, B. Li, et al., "A study of mode I delamination resistance of a thermoplastic composite," *Compos. Sci. Technol.*, **45**, 173–179 (1992).

Received 03. 07. 2014